Metallurgy and Foundry Engineering – Vol. 41, 2015, No. 2, pp. 85–98
http://dx.doi.org/10.7494/mafe.2015.41.2.85

**Mohsin Raza, Roger Svenningsson, Mark Irwin**

# Experimental study of the filling of thin-walled investment castings in 17-4PH stainless steel

## Badania doświadczalne wypełniania form ceramicznych cienkościennych odlewów ze stali nierdzewnej 17-4PH

**Abstract**
Global requirements of lower fuel consumption and fewer emissions are increasing the demand for decreasing the weight of cast components. Reducing the wall thickness of cast components is one way of achieving this. The aim of this work was to investigate castability of 17-4PH stainless steel in thin-walled test geometries (≤2 mm). The casting trials were performed to investigate fluidity as a function of casting temperature, mold preheat temperature, and filling systems in thin-walled sections. It was observed that fluidity in a top-gated configuration is strongly affected by casting temperatures; however, the effect of mold preheat temperature on fluidity was not significant. On the other hand, castings made in bottom-gated configuration were more stable, and fluidity was not significantly affected by variation in casting temperature and mold preheat temperature. Fewer porosity and flow-related defects were observed in the bottom-gated system as compared to the top-gated one.

**Keywords:** investment casting, fluidity, thin sections, porosity, 17-4PH

**Streszczenie**
Światowe wymagania niższego zużycia paliw i mniejszej emisji gazów powodują wzrost zapotrzebowowania na wyroby odlewane o mniejszej wadze. Zmniejszenie grubości ścianki odlewów jest jedną z metod spełnienia tego założenia. Celem niniejszej pracy jest badanie lejności stali nierdzewnej 17-4PH w próbach o cienkościennej geometrii (≤2 mm). Badania odlewania zostały przeprowadzone w celu przeanalizowania lejności w funkcji temperatury zalewania, temperatury nagrzania formy oraz cienkościennych przekrojów elementów układu wlewowego. Zaobserwowano, że w przypadku górnego układu wlewowego temperartura zalewania ma duży wpływ na lejność, jednakże wpływ temperatury nagrzania formy na lejność był nieznaczny. Z kolei odlewy

**Mohsin Raza M.Sc. Eng.:** Mälardalen University, Eskilstuna, Sweden, TPC Components AB, Hallstahammar, Sweden; **Roger Svenningsson M.Sc. Eng.:** Swerea SWECAST, Jönköping, Sweden; **Mark Irwin Ph.D.:** TPC Components AB, Hallstahammar, Sweden

otrzymane w konfiguracji z dolnym układem zalewania były bardziej stabilne, a różne temperatury zalewania oraz temperatury nagrzania formy nieznacznie wpłynęły na lejność. Zaobserwowano mniejszą porowatość oraz mniejszą ilość wad przy zastosowaniu dolnego układu wlewowego w porównaniu z górnym układem wlewowym.

**Słowa kluczowe:** odlewanie precyzyjne w formach ceramicznych, lejność, odlewy cienkościenne, porowatość, 17-4PH

## 1. Introduction

In order to investigate the castability of alloys in thin-walled geometries, the mechanism behind fluidity (in terms of flowability and fillability) is important to understand. Generally, the literature available on this topic is based on investigations related to measurement of fluidity length as a function of either alloy composition or process parameters such as casting temperature and shell preheat temperature. The influence of parameters related to alloy, mold, and pouring in relation to fluidity are summarized in the literature [1]. The influence of superheating the melt on fluidity is well-documented in the literature, and a linear relation is often presented [1–3]. Correspondingly, an increase in the heat of fusion can contribute to an increase in fluidity [1, 4]. Many studies [1, 5–7] present a linear relationship between mold temperature and fluidity that can be explained by a lower temperature difference between the alloy and the heated mold (which delays freezing). However, there are also studies that show a non-linear relation or no influence of an increase in mold temperature [6, 8, 9]. Pressure head is yet another well-documented parameter that affects both flowability and fillability [1, 4]. Often, a linear relation between pressure head and fluidity is reported [1, 7, 10, 11]. By using vibration- or vacuum-assisted casting, the effective pressure head can be increased; hence, improving fluidity [7, 12–15]. The effect of filling mode that is top filling or bottom filling are also well-documented in terms of the quality of castings [16, 17]. It has been previously presented in the literature that bottom filling is beneficial in terms of porosity [16]. This study focuses on exploring the effects of casting conditions on the castability of a test geometry taken from a gas turbine component using a 17-4PH alloy (an aerospace-grade stainless steel). The results of the study will be further used to produce lightweight turbine components. In this study, existing knowledge on the topic has been applied to produce a thin-walled section of a turbine component by varying the foundry parameters; i.e., casting temperature, mold preheat temperature, and mode of filling. The results from the study are evaluated in terms of fluidity, porosity, and flow-related defects in the castings.

## 2. Experimental work

To study the effects of casting parameters on fluidity and quality of castings, geometries with two different thicknesses (i.e., 1.5 mm and 2 mm) were assembled using both conventional top- and bottom-gated runner systems. The test geometry used was a curved blade

of 100 × 150 mm with a base of 120 × 20 × 20 mm. In order to establish a relationship between casting parameters and fluidity of 17-4PH, a set of experiments was designed. The parameters studied were superheat, mold preheat temperature, thickness of test geometry, and mode of filling. Casting were made in air using a high-frequency furnace.

## 2.1. Geometry and gating system

Both top-down pouring (top-gated filling) and bottom-up pouring (bottom-gated filling) were performed in the casting trials. The principle for the set-up is shown schematically in Figure 1a, b. The sprue used in the cluster design of the bottom-gated system was 300 mm high with a diameter of 40 mm. The pouring cup attached to the sprue was 125 mm high and 125/60 mm in diameter for both the top-gated and bottom-gated systems. For both filling systems, the runners used were 40 × 40 mm in the cross-section. The gating was designed so that the entire cross-section of the base of the blade was attached to the runners. No additional feeders were used. Test geometries were mounted on runner systems (clusters) both in the top-gated and bottom-gated configurations. Vents were provided on all clusters in order to facilitate air removal from the mold during pouring.

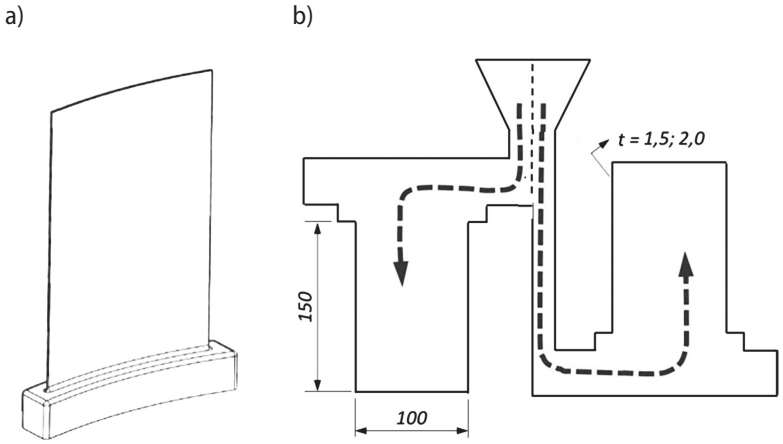


*Fig. 1. Illustrating sample test geometry and filling modes: a) casting geometry; b) gating principles, top- and bottom-gated runner system*

## 2.2. Mold manufacturing

Ceramic molds were produced following standard foundry procedures by continuously dipping and stuccoing the wax assemblies until the desired 6–8 mm shell thickness was achieved. For prime layers, a colloidal silica slurry was used with a 325–200 mesh zircon flour. Aluminium oxide (with a mesh size ranging from 90–54) was used to coat the slurry. For back-up layers, colloidal silica with a 200-mesh aluminium silicate slurry was used. Aluminium silicate with a 16–30 mesh was used for stuccoing the backup layers.

After drying, the shells were placed in an autoclave for de-waxing. In order to harden the shells, sintering was performed. The shells were preheated in a push-through furnace for a minimum of two hours before castings.

To produce data for simulation work, thermal properties of the ceramic mold and thermodynamic data for 17-4PH were also collected.

## 2.3. Cast alloy

*Table 1. Composition of cast alloy*

| Element | Fe | C | Si | Mn | P | S | Cr | Ni | Cu | Nb | N |
|---|---|---|---|---|---|---|---|---|---|---|---|
| Content (wt %) | Bal | 0.042 | 0.72 | 0.60 | 0.014 | 0.014 | 16.36 | 3.73 | 3.1 | 0.042 | 0.057 |

ASTM A747 (a castable alloy analogous to precipitation-hardening stainless steel 17-4PH with a composition as shown in Table 1) was used for the casting trials. Before the trials, a thermal analysis was carried out to establish the liquidus temperature of the alloy. Based on these temperature measurements, the liquidus temperature was estimated to be 1462°C.

## 2.4. Test plan for castability measurements

Casting trials were performed according to Table 2. All castings were performed in air. As the trials were performed under production-like conditions, variations related to the alloy composition were assumed to be negligible in comparison to the other parameters; therefore, they were neglected. Two casting parameters (i.e., shell temperature and casting temperature) were analyzed with respect to the two feeding systems (i.e., bottom filling and top filling). The temperature drop in the shell during transportation between the preheating oven and casting furnace was also recorded to evaluate variations in shell temperature. At the time of pouring, the internal temperature of the mold was also measured, in order to relate the actual mold temperature to the fluidity measurements. Using a conventional thermal imaging camera, the pouring process for each casting was filmed to estimate and verify pouring time, mold temperature, and melt temperature at the time of pouring. Four clusters were manufactured for each casting set-up, giving total of 32 clusters with a total of 64 geometries.

*Table 2: Test plan for test geometries*

| Test set-up | Mold temp. [°C] | Pouring temp. [°C] | Filling direction |
|---|---|---|---|
| No. 1 | 900 | 1550 | top-gated |
| No. 2 | 900 | 1550 | bottom-gated |

*Table 2 cont.*

| | | | |
|---|---|---|---|
| No. 3 | 1100 | 1550 | top-gated |
| No. 4 | 1100 | 1550 | bottom-gated |
| No. 5 | 900 | 1700 | top-gated |
| No. 6 | 900 | 1700 | bottom-gated |
| No. 7 | 1100 | 1700 | top-gated |
| No. 8 | 1100 | 1700 | bottom-gated |

## 3. Results

Test results were evaluated in terms of filled areas in the 1.5 mm and 2 mm geometries. As the drop in temperature in the shell is not constant over time, it is important to relate the actual shell temperature to the filled area at the time of casting. The temperature vs. time graph in Figure 2 shows rapid cooling immediately after the shell is removed from the preheat furnace. Microporosity- and flow-related defects were also evaluated to understand the effect of the filling system on castability.

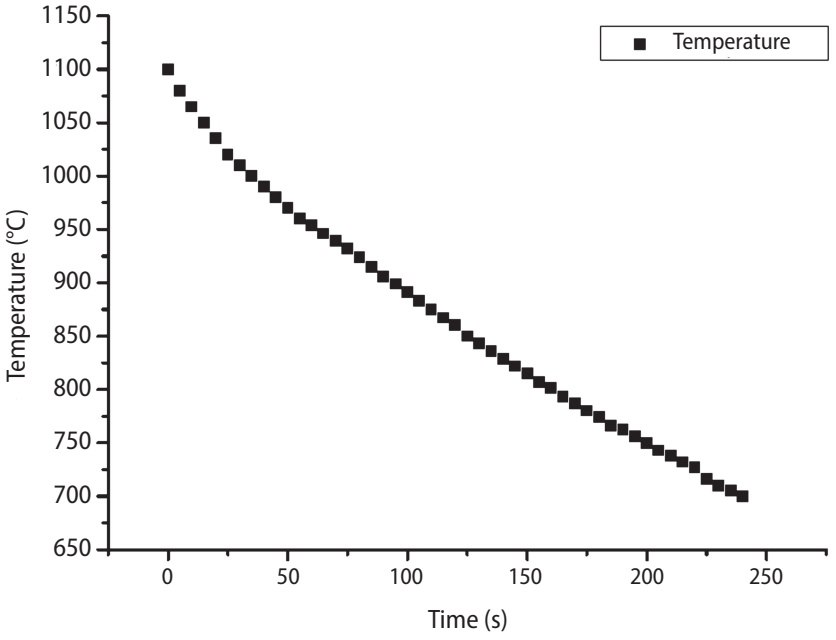


*Fig. 2. Illustrates temperature drop inside the shell during transport*

## 3.1. Fluid behavior

A distinctive difference in flow pattern was observed when comparing the top- and bottom-gated runner systems. For the top-gated system, a non-uniform filling occurred over the width of the blade which resulted in an *unzipping* [18] type of propagation of the melt. For the bottom-gated system however, where the metal flow was in an up-ward direction (i.e., moving opposite to gravity), no *unzipping* type of propagation was observed. For both the top- and bottom-gated geometries, it was observed that the extent of filling was greater along the edges of the mold cavity. These differences between the top- and bottom-gated runner systems appeared to be valid for all casting trials.

## 3.2. Effects of process parameters

In Figures 3–6 typical fluidity results are shown. Figure 3 compares the fluidity results in 1.5 mm-thick geometry cast at two different temperatures (i.e., 1700°C and 1550°C) according to the set-up shown in Table 2. A significant increase in filling in the geometry was observed at 1700°C when compared to the 1500°C. As discussed in previous section, non-uniform filling was observed in both geometries.

Figure 4 shows the effect of the mold preheat temperature on the filling in the 1.5 mm-thick geometry. It was observed that mold preheat temperature does not significantly effect mold fillability.

Figure 5 compares the top-filling and bottom-filling systems in the 1.5 mm test geometry. A more-regular filling front was observed in bottom-filling compared to the top-filling system; however, more filling at the edges of each geometry was observed in both filling systems. Similar results from the 2 mm test geometry are shown in Figure 6.

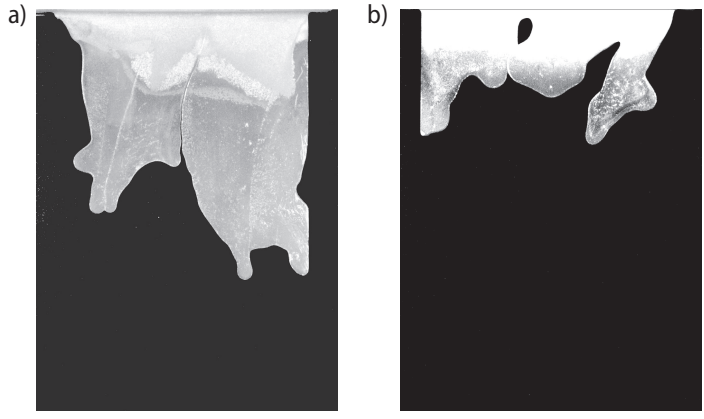


*Fig. 3. Effect of casting temperature on fluidity: a) setup 5–1.5 mm, top gated, $T_{POUR}$ 1700°C, $T_{mold}$ 900°C; b) setup 1–1.5 mm, top gated, $T_{POUR}$ 1550°C, $T_{mold}$ 900°C*

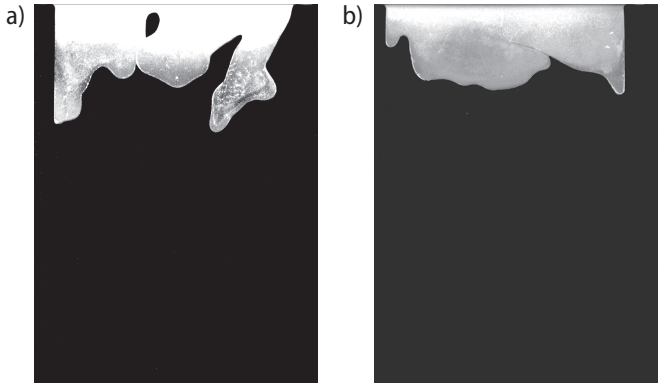


*Fig. 4. Effect of shell temperature on fluidity: a) setup 1–1.5 mm, top gated, $T_{POUR}$ 1550°C, $T_{mold}$ 900°C; b) setup 3–1.5 mm, top gated, $T_{POUR}$ 1550°C, $T_{mold}$ 1100°C*

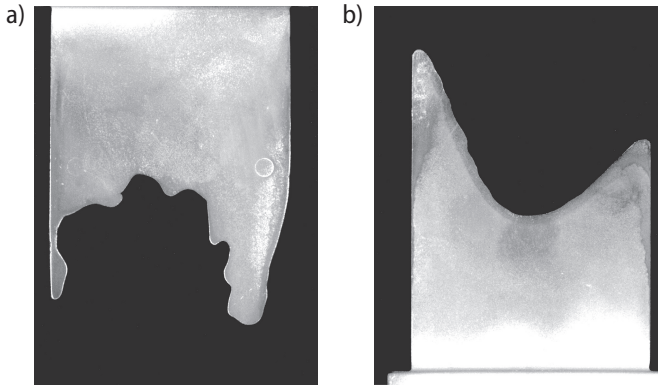


*Fig. 5. Comparison of fluidity between top-gated and bottom-gated: a) setup 7–1.5 mm, top gated, $T_{POUR}$ 1700°C, $T_{mold}$ 1100°C; b) setup 8–1.5 mm, bottom gated, $T_{POUR}$ 1700°C, $T_{mold}$ 1100°C*

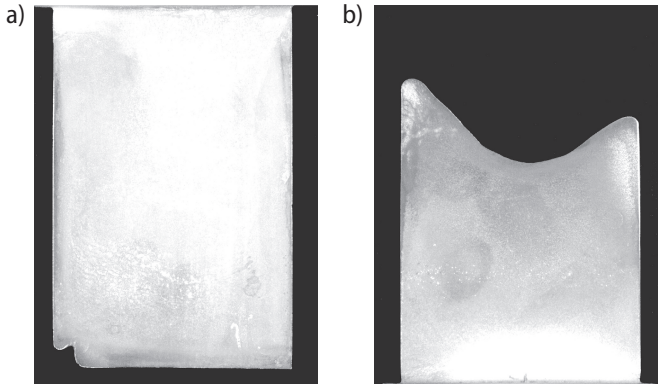


*Fig. 6. Comparison of fluidity between top-gated and bottom-gated: setup 7–2 mm, top gated, $T_{POUR}$ 1700°C, $T_{mold}$ 1100°C; b) setup 8–2 mm, bottom gated, $T_{POUR}$ 1700°C, $T_{mold}$ 1100°C*

The normalized filled area was calculated by digital image processing and used as a measure of filling, ranging from 0.0 to 1.0. A schematic illustration is shown in Figure 7. The area calculation was performed on the open-source software ImageJ [19]. A completely filled blade corresponding to a fluidity of 1.0 was used as reference. In Figure 8, fluidity results are compared between top-gated and bottom-gated runner systems, along with the deviation of each trial for blade thicknesses of 1.5 and 2.0 mm. Even though the deviation is large for both casting systems, the results show that the top-gated system offers increased fluidity compared to the bottom-gated one. It is also observed that the casting temperature at both thicknesses has a significant effect on fluidity (as shown in Figures 3, 6, and 9) while shell temperature does not appeared to be significant (see Figures 4 and 9). Fluidity is less affected by geometry thickness in the top-gated geometry as compared to the casting temperature, which was opposite in the bottom-gated system (as shown in Figure 9). Figure 9 also shows that fluidity is not significantly affected by shell transportation time within the experimental set-up range.

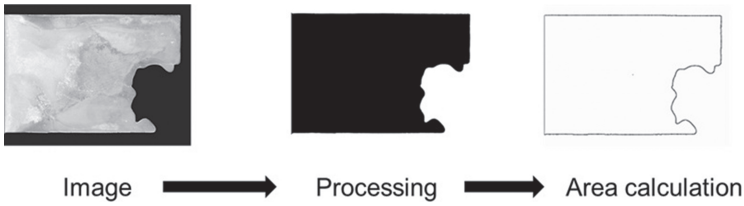


*Fig. 7. Illustrates evaluation technique of projected area*

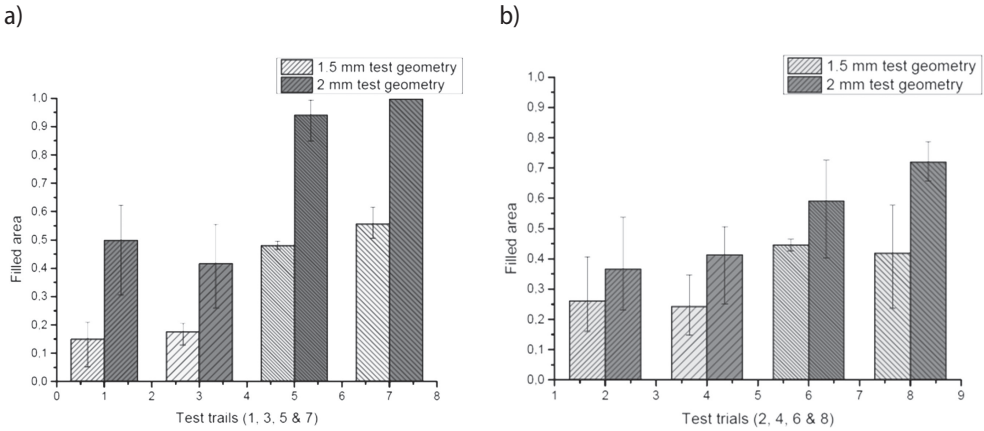


*Fig. 8. Fluidity results for each set up; light gray bars = 1.5 mm and dark gray bars = 2.0 mm: a) top-gated runner system; b) bottom-gated runner system*

a) b)

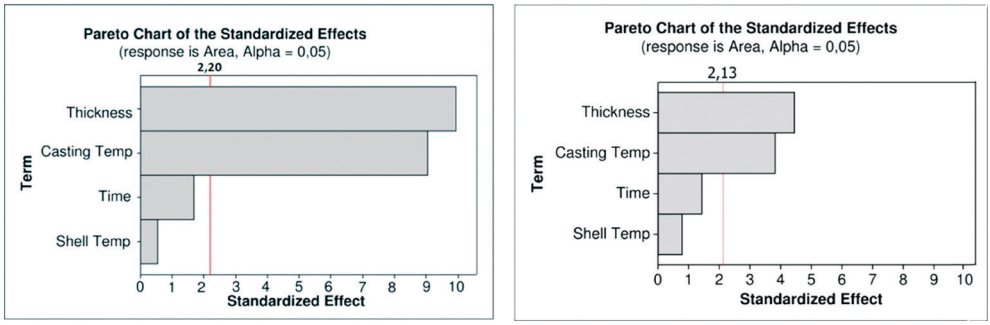


*Fig. 9. Effect of parameters for 1.5 mm and 2.0 mm test geometries: a) top-gated runner system; b) bottom-gated runner system*

## 3.3. Porosity in thin sections

Porosity was evaluated by means of dye-penetrant testing. Results from the penetrant testing are shown in Figure 10. As can be seen, the top-gated castings exhibit several large pores close to the surface while the bottom-gated castings appear to be free from such pores. A slight overall tint, however, is seen for all samples, indicating microporosity. In order to get a rough estimate of the size of porosity and its nature, the samples were cut from six equally distanced sections from bottom to top of the blade and analyzed using light optical microscopy (LOM). Microscopic analysis was only performed for shrinkage pores. Gas pores were not analysed in this work. The bulk sample (represented by "0" in Figure 11) was taken from the thicker base of the blade.

a) b)

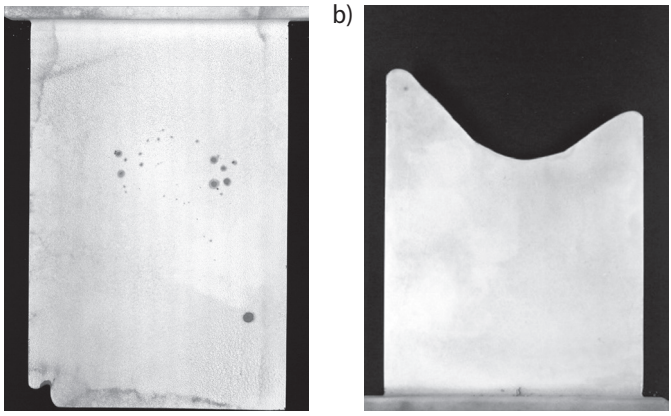

*Fig. 10. Penetrant results for 2 mm thickness: a) setup 7–2 mm, top gated, $T_{POUR}$ 1700°C, $T_{mold}$ 1100°C; b) setup 8–2 mm, bottom gated, $T_{POUR}$ 1700°C, $T_{mold}$ 1100°C*

Figure 11 shows the distribution of porosity for 2 mm blades from three different set-ups, giving the comparison between top-gated and bottom-gated systems. Porosity investigations were performed along the center of each section using LOM. The average porosity of the samples was determined as an area fraction of the investigated surface, taking an average of five measurements in 110× or 180× magnification. The uneven distribution of porosity in samples from Set-up 7 is due to the sudden appearance of a number of large pores.

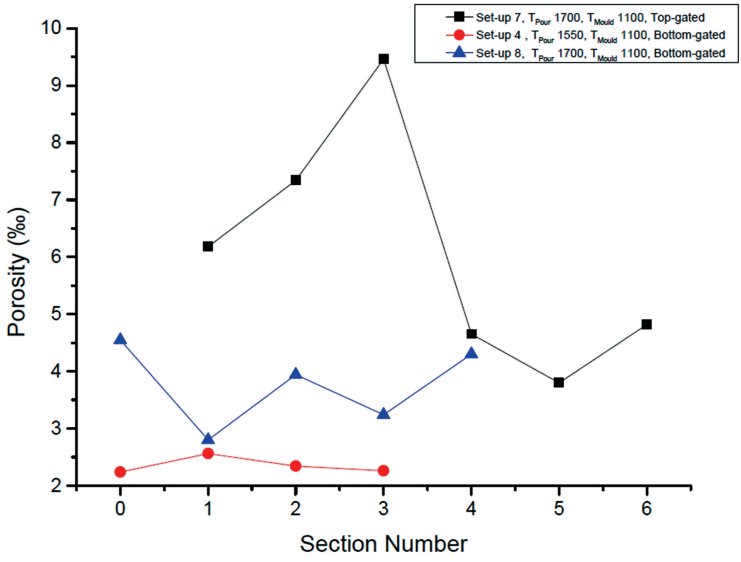


*Fig. 11. Average porosity expressed as area fraction of pores for the investigated samples*

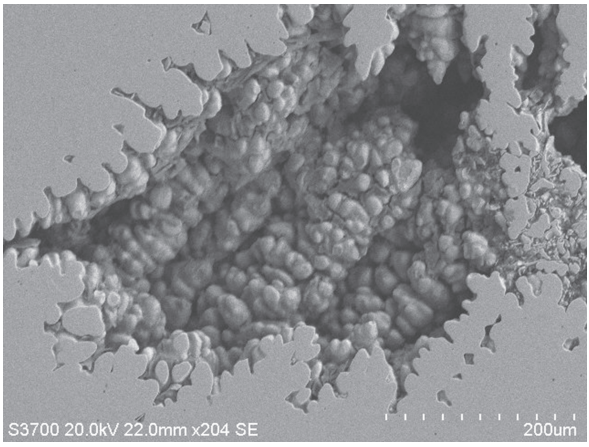


*Fig. 12. SEM images showing large shrinkage pores in top-gated sample from Set-up 7*

The selected samples were further investigated using scanning electron microscopy (SEM) in order to understand the porosity-formation mechanism. Figure 12 shows large shrinkages pores in a SEM image for cut-up section 3, Set-up 7 presented in Figure 11.

## 4. Discussion

It was observed that casting temperature has a significant impact on the fluidity of 17-4PH for the casting of a test blade in both top-gated and bottom-gated systems (as shown in Figures 3, 8, and 9). However, fluidity was not significantly affected by mold temperature in castings regardless of their gating systems (as shown in Figures 4 and 9). This might be attributed to the fact that, due to the delay in pouring during transportation and pouring preparation, the shell temperature had already dropped significantly. It is important to consider that the 1100°C shells cooled more rapidly due to stronger radiation losses as compared to the 900°C shells.

In the top-gated system, the effect of surface tension was more pronounced (see Figure 5). As the metal flow during top-gated filling is turbulent, a solid film rapidly forms on the surface of the flowing metal stream. Due to friction, the solidified film is pinned to the walls of the cavity while a new solid layer continues to form at the surface of the flowing stream. The pinning effect causes splits at the surface of the flowing stream, allowing the metal stream to flow only along the strong chains of solid films. The liquid stream will keep flowing as long as the velocity of the liquid and pressure head are sufficient to break the surface film [18]. This phenomenon (which was clearly observed in the top-gated system) is described as an *unzipping* type of propagation in the results section. In the bottom-gated system, however, the melt propagation was smoother. It was also observed in both top-gated and bottom-gated systems that, due to the thermal expansion of the ceramic shell, the vertical edges of the geometry were cracked and opened-up, resulting in an increase in thickness at the edges as compared to the center of the mold cavity. The capillary repulsion in the thinner channel stops metal flow and diverts it to the thicker areas (where capillary repulsion is lower [18]). The phenomenon is shown in Figures 5 and 6, where more filling on the edges of geometry is observed.

Turbulent flow in the top-gated system also causes porosity and shrinkage. A high level of porosity was observed in the top-gated system as compared to the bottom-gated one (as presented in Figures 10 and 11). Figure 11 shows that castings from Set-up 7 (which is top-gated) have more porosity than those from Set-ups 4 and 8 (which are bottom filled). These results are supported by the previous work [16, 17], in which it is shown that the level of porosity and inclusions are higher for top-gated systems compared to bottom-gated systems. The difference in porosity levels between castings from Set-ups 4 and 8 seems to be dependent on casting temperature. In the

castings made at increased casting temperatures, more shrinkage pores are observed. A higher temperature difference between metal and mold results in higher shrinkage and gas pores [20]. For the bottom-gated casting system, the velocity of the melt into the thin cavity is controlled by the inlet system. Also, the molten metal moves upward, forming a planar smooth surface and thereby not exposed to air (except at the flow tip). For the top-gated system, however, the filling is uncontrolled, and the metal enters the cavity in a non-uniform way (i.e., metal is exposed to air that could result in bi-oxide films, later acting as nucleation sites for pores). Furthermore, uncontrolled filling could potentially entrap a great amount of air, which may not be evacuated during solidification. At higher temperatures, air has a higher solubility in the melt; thus, the entrapment of oxides is aggravated in the case of turbulent filling.

The penetrant testing showed large differences between top- and bottom-gated castings with respect to the amount of large shrinkage pores close to the surface. The average porosity of the heat-treated samples thus varied from 2‰ for the bottom-gated system to almost 10‰ for the top-gated system. A remarkably large degree of porosity defects for the top-gated 2 mm blades at high metal temperature were observed. However, no difference was observed between the top-gated and bottom-gated systems in terms of porosity for the lower melt temperature. The authors also observed that cross-sectional analysis of the geometries creates a large uncertainty, since it examines only a small fraction of the cast volume. To get a picture of the overall porosity, total X-ray scanning of all castings was performed; however, the results have not been quantified in this work. Similarly, porosity due to the entraped air in the mold is also not analyzed in this work.

Generally, the top-gated casting system showed a better filling compared to the bottom-gated system for the test geometry used in this work. Melt temperature appeared to be the most significant casting parameter in terms of filling, followed by the thickness of the mold cavity for the top-gated system. However, for the bottom-gated system, mold thickness was more significant than casting temperature. The results from the work provides the knowledge about castability of 17-4PH in thin-sections for turbine components. However, there is a certain margin of error in direct comparison of the bottom- and top-gated geometries due to small differences in the design of the gating system. It is important to note that the gating system used in this experimental work has a much longer sprue length for the bottom-gated casting than the top-gated one. This gives the metal more time to cool before entering the bottom-gated geometry, as well as a larger pressure head. Both of these factors might have affected the filled area. It would have been better to have the top-gated runner coming off of the bottom of the sprue instead of the top. Although vents were provided to facilitate air removal from the mold, a different length of sprue for the top- and bottom-gated systems (and thus, the amount of air in the sprue) might have an effect on gas porosity (which was not analyzed in this work).

## 5. Conclusions

- Both melt temperature and thickness of the mold cavity had a larger impact on fluidity for the top-gated system as compared to the bottom-gated one.
- The bottom-gated system is more stable and is not significantly effected by casting parameters (i.e., casting temperature and mold-preheat temperature).
- Mold-preheat temperature does not appear to be significant in terms of its effect on fluidity.
- A high level of porosity was observed in the castings made in the top-gated configuration as compared to the castings in the bottom-gated one.
- High pouring temperatures resulted in more shrinkage-related defects regardless of the filling system.


### Acknowledgement

This work has been supported by the CleanSky Joint Undertaking project "LEAN - Development of lightweight steel castings for efficient aircraft engines "Project No. 296585." The authors gratefully acknowledge the comments and suggestions received from Jon A. Dantzig, Sten Farre, and Åsa Lauenstein. The authors also thankfully acknowledge the financial support of the Innofacture Program at Mälardalens Högskola, funded through KK-Stiftelsen.


### References


[1] Capadona J., Albright D.: Review of fluidity testing as applied to lostpolystyrene investment castings. AFS Transactions, (1978), 43–54

[2] Campbell J., Oliff I.: Static and dynamic criteria for filling of thin section molds. AFS Cast Metals Research Journal, 7 (1971), 55–61,

[3] Campell J.: Thin walled castings. Material Science and Technology, 4 (1998), 194–204

[4] Flemings M.: Fluidity of metals – techniques for producing ultra-thin sections castings. The British Foundryman, 57 (1964), 312–325

[5] Walker B.: New type of fluidity test piece. Foundry Trade Journal, 115 (1963), 713–721

[6] Chandraseckariah H.S., Seshan S.: Effect of foundry variables on fluidity of investment cast nickel-base super alloys. Transactions of the American Foundry Society, 110 (2002), 681–695

[7] Lun Sin S., Dubé D.: Influence of process parameters on fluidity of investmentcast AZ91D magnesium alloy. Material Science and Engineering A, 386, 1–2 (2004), 34–42

[8] Magurie M.C., Zanner F.J., Minteer D.J., Murray J.D.: Gating gemotry studies of thin-walled 17-4PH investment castings. 40th Annual Technical Meeting, Investment Casting Institute, Las Vegas, 1992

[9] Olliff I.D., Lumby R.J., Kondic V.: Some new ideas on fluidity test mold desig. Foundry, 93 (1965), 80–85

[10] Flemings M., Mollard F., Niiyama E.: Fluidity of aluminium. AFS Transactions, 70 (1962), 1029–1039

[11] Campell J.: Castings. Butterworth-Heinemann, Oxford – Massachusetts ,1993.

[12] Abdul-Karem W., Al-Raheem K.F.: Vibration improved the fluidity of aluminium alloys in thin walled investment casting. International Journal of Engineering, Science and Technology, 3 (2011), 120–135

[13] Vainer M., Lerner Y.: Vacuum-assisted investment casting of Al-Ni-Bronze. Transactions of the American Foundrymen's Society, 107 (1999), 35–42
[14] Matsuna K., Ohama S.: Application of the investment casting method for extremely thin blade impellers. Ishikawajima-Harima Engineering, 21 (1981), 45– 50
[15] Chandley G., Cargill D.: Thin-walled castings by the CLV process. Transactions of the American Foundrymen's Society, 98 (1990), 413–416
[16] Li D.Z., Campell J., Li Y.Y: Filling systems for investment cast Ni-base turbine blades. Journal of Materials Processing Technology, 148, 3 (2004), 310–316
[17] Lun Sin S., Dubé D., Tremblay R.: An investigation on microstructural and mechanical properties of solid mould investment casting of AZ91D magnesium alloy. Material Characterization, 59, 2 (2008), 178–187
[18] Campbell J.: Complete Casting Handbook: Metal Casting Processes, Metallurgy, Techniques and Design. Elsevier, 2011
[19] Rasband W.S.: ImageJ. U.S. National Institutes of Health, Bethesda, Maryland, http://imagej.nih.gov/ij/, 1997–2014
[20] Dantzig J.A., Rappaz M.: Solidification. FPFL Press, 2009